ISSN 1990-7931, Russian Journal of Physical Chemistry B, 2018, Vol. 12, No. 1, pp. 108–114. © Pleiades Publishing, Ltd., 2018.
Original Russian Text © N.G. Bykova, I.E. Zabelinskii, L.B. Ibragimova, P.V. Kozlov, S.V. Stovbun, A.M. Tereza, O.P. Shatalov, 2018, published in Khimicheskaya Fizika, 2018, Vol. 37, No. 2, pp. 35–41.

COMBUSTION, EXPLOSION, AND SHOCK WAVES

Radiation Characteristics of Air in the Ultraviolet and Vacuum Ultraviolet Regions of the Spectrum behind the Front of Strong Shock Waves

N. G. Bykova[a], I. E. Zabelinskii[a], L. B. Ibragimova[a], P. V. Kozlov[a], S. V. Stovbun[b], A. M. Tereza[b], and O. P. Shatalov[a, *]

[a] *Institute of Mechanics, Moscow State University, Moscow, 117192 Russia*
[b] *Semenov Institute of Chemical Physics, Russian Academy of Sciences, Moscow, 119991 Russia*
**e-mail: shatalov@imec.msu.ru*

Received May 26, 2017

Abstract—Experiments on the measurement of air emission intensity behind the front of incident shock wave were carried out in a shock tube at an initial pressure of 0.25 Torr and shock wave velocities of 6.3–8.4 km/s. The emission intensity was measured in absolute units both in the form of an integral spectral distribution in a wavelength range of 120–400 nm (panoramic spectra) and as the time evolution of emission at the individual atomic lines of nitrogen and oxygen atoms. The results of the measurements demonstrated that the emission in air behind a shock wave in the vacuum ultraviolet region of 120–200 nm had a much higher radiation flux level than the emission in a range of 200–900 nm.

Keywords: shock waves, vacuum ultraviolet, emission spectroscopic measurements
DOI: 10.1134/S1990793118010165

INTRODUCTION

A number of studies oriented to the measurement of radiation fluxes behind a shock wave front over a wide range of wavelengths at low initial pressures and high speeds were initiated because of the need for taking into account the radiation heating of a descent module due to the emission of gas [1–4]. Those studies are currently in progress. In particular, Johnston [4] listed five experimental installations that operate in Europe, Japan, Australia, and the United States in order to investigate the emission of gas in a range of 120–200 nm for the simulation of radiation flux in a flow around a spacecraft that enters the Earth's atmosphere. He obtained an integral radiation power distribution and the time evolution of air at an equilibrium temperature from 9900 to 12400 K in the emitting layer.

Different models were proposed [5–9] for the quantitative description of radiation fluxes. In this work, we report the results of the measurements of the integral and time characteristics of the emission of air heated in shock wave in the vacuum ultraviolet (VUV), ultraviolet, and visible regions of the spectrum. It is well known that, at high shock wave velocities, the radiated power in the VUV region is much higher than that in the visible region [2]. In connection with this, the data on the time evolution of emission behind the shock wave front were primarily obtained in the VUV region. These data differ from analogous results, for example, published by Grinstead et al. [1], in terms of the fact that the emission was recorded in narrower spectral intervals; this made it possible to separately observe the evolution of emission from different energy levels of N and O atoms (or atomic ions), which are the basic components of high-temperature air.

The aim of this work was to obtain experimental data on the integral emission of air in a short-wave region of the spectrum and on the time evolution of the emission of the atomic components of air behind the front of strong shock waves.

EXPERIMENTAL

The emission intensity measurements were performed in a shock tube (Fig. 1). The inner diameter of the tube was $d = 50$ mm. Oil-free vacuum pumps (an Alcatel Drytel 1025 vacuum pumping system with forvacuum pumping using an ISP–250C pump from Anest Iwata) were used for the evacuation of the shock tube, a vacuum monochromator, and supply lines. Shock wave generation was performed on the ignition of a stoichiometric mixture of oxygen with hydrogen diluted by helium (to 70%) in a high-pressure chamber (HPC). The total pressure of the mixture in the HPC varied from 4 to 10 atm. A low-pressure chamber (LPC) was filled with the test gas to a pressure of

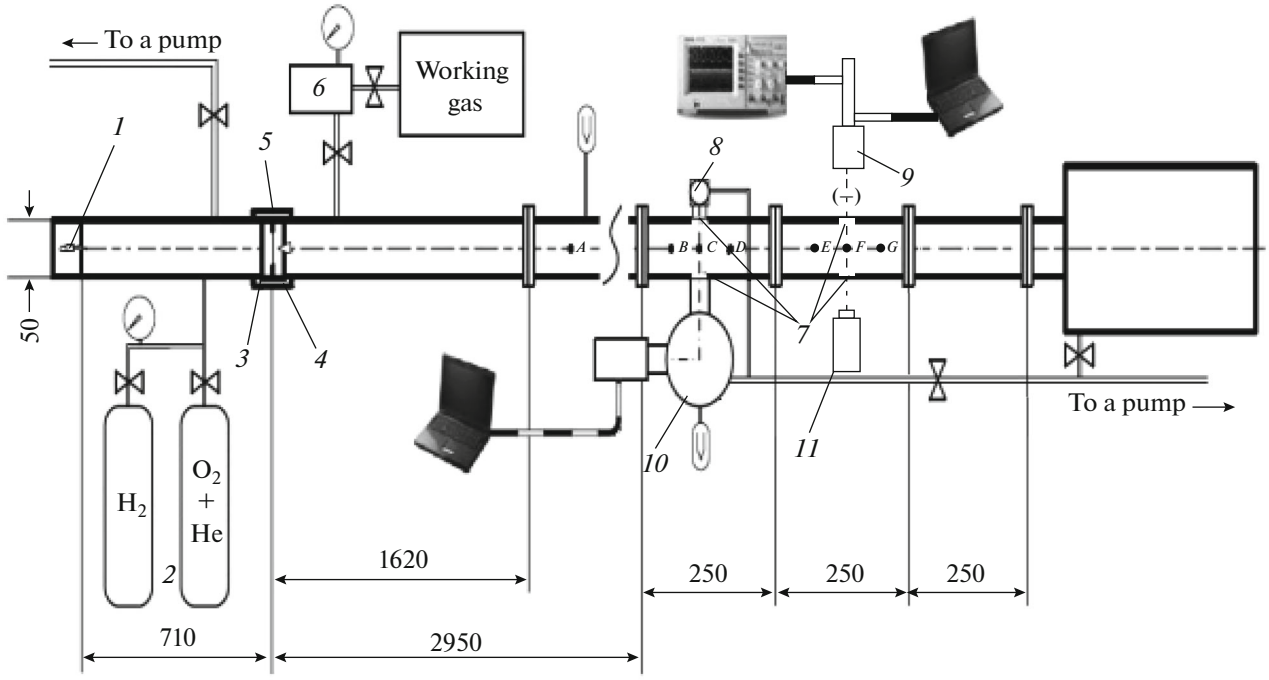

Fig. 1. Schematic diagram of the installation: (*1*) spark plug in the high-pressure chamber, (*2*) high-pressure gas cylinders, (*3–5*) diaphragm unit, (*6*) working gas inlet system, (*7*) optical windows, (*8*) standard deuterium lamp, (*9, 10*) spectroscopic instruments with the detection system (photomultiplier tube and CCD cameras), and (*11*) laser for adjustment. The positions of pressure sensors are designated by the letters *A–G*. The sizes are given in mm.

0.25 Torr. The inleakage of air as a result of faulty sealing and gas desorption from the pipe walls was no greater than 4×10^{-4} Torr/min. Oxygen with a purity of 99.999% and nitrogen with a purity of 99.996% were used in the experiments. The rupture of a diaphragm that separates the HPC and LPC leads to shock wave propagation along the LPC channel. The shock wave velocity wave was measured with the aid of piezoelectric detectors. The measuring section of the shock tube was used for the detection of emission in the VUV region.

Figure 2 shows the optical arrangement of measurements for the detection of emission in the VUV region in the measuring section. A VM-1 vacuum monochromator together with vacuum channel *6* were connected with the shock tube and pumped out with an oil-free pump. The width and height of optical slit *5* in the tube wall were 0.3 and 8 mm, respectively. The width and height of the entrance slit of the monochromator were $S = 0.1$ mm and $h = 10$ mm, respectively. Calibrated radiation source *1* was mounted on the other side of the shock tube in the pumped-out volume. An L879–01 deuterium lamp from Hamamatsu was used as this source. The radiation detector (position *9* in Fig. 2) was either a Lega charge coupled device (CCD) camera for measuring the spectral distribution of emission (panoramic spectra) in a range of 115–400 nm or a photomultiplier tube for detecting the time evolution of emission behind a shock wave front. Photomultiplier tubes from Hamamatsu sensitive in the regions of 115–320 and 120–180 nm were used. The diffraction grating of a monochromator with 600 lines/mm (linear dispersion, ~35 Å/mm) made it possible to separate narrow regions of the spectrum (with a width of 1–1.5 nm) in the regions of wavelengths corresponding to atomic lines.

The shock wave velocity was determined by signals from two sensors located at a distance of 100 mm from each other symmetrically on both sides of the axis of optical measurements. The middle sensor was located in the middle between them in a section with the optical axis of the radiation detection system. Subsequently, the beginning of a sharp increase in the signal from this sensor was chosen as a reference point for zero time in the detection of the evolution of emission.

CALIBRATION OF THE OPTICAL SYSTEM

The Lega camera, which was used for the measurement of the panoramic emission spectra of shock waves in the vacuum ultraviolet region, consisted of an image converter with an MgF_2 input window and a CCD matrix. The spectral sensitivity range was 115–850 nm. The camera was placed in a focal plane at the monochromator output. The size of the matrix was 10 × 20 mm; therefore, a region of the spectrum ~70 nm in

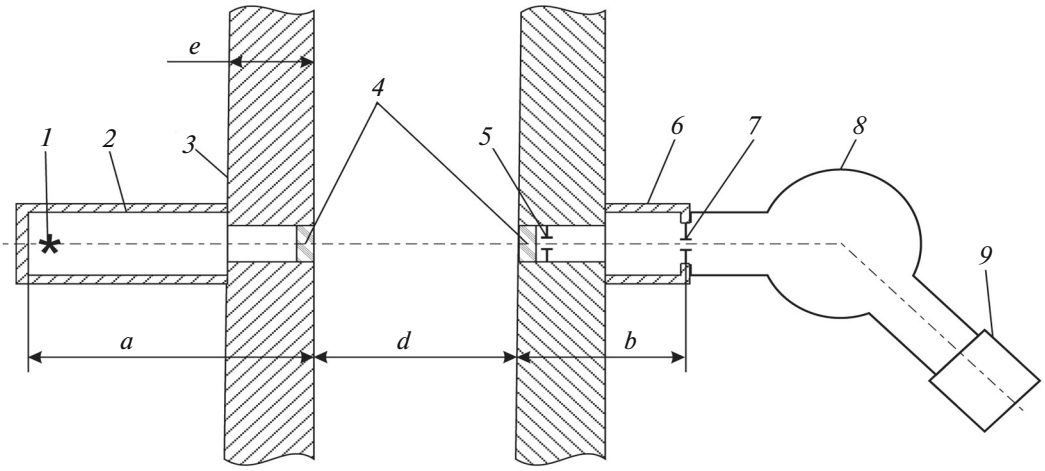

Fig. 2. Optical measurement and calibration system on the UTS shock tube: (*1*) calibrated radiation source, (*2, 6*) connector vacuum channels, (*3*) shock tube body, (*4*) optical windows of MgF_2, (*5*) optical slit on the shock tube, (*7*) optical slit at the monochromator inlet, (*8*) VM-1 vacuum monochromator, and (*9*) radiation detector (CCD camera or photomultiplier tube); $a = 70$ mm and $b = 210$ mm.

width was detected in an experiment at the monochromator dispersion of ~35 Å/mm. In the experiments, we have restricted ourselves to a section of 50 nm and measured spectra with a step of 20–30 nm (with superimposition). The width of instrument function in the experiments was 1.5 nm.

The spectral sensitivity of the optical system was calibrated by a comparison with the spectrum of a calibrated source; a deuterium lamp is commonly used as this source in the VUV region of the spectrum. In the course of the calibration, a monochromator and recording equipment were arranged on the one side of the shock tube, whereas a deuterium lamp was mounted on the other side (Fig. 2). The lamp was mounted in an airtight manner in order to ensure a necessary vacuum level in the path of the radiation; in this case, an optical window on the side of the lamp was demounted from the shock tube to exclude additional losses in the calibration circuit. Differences in the geometry of the optical calibration circuit and the measuring circuit were taken into consideration in the calculation of a calibration curve.

Figure 3 shows a graph of the spectral radiance of deuterium lamp emission (curve *1*) converted to an instrument function width of 1.5 nm, which corresponds to the experimental conditions, and the spectra of calibration measurements (curves *2* and *3*) measured with the Lega camera. Based on these data, we obtained a calibration function of the optical system, which was used subsequently in the conversion of data on the spectral radiance of UV emission into absolute energy units. Figure 4 shows the emission spectra of an air mixture in a shock wave at the initial pressure $p_1 = 0.25$ Torr in the LPC in arbitrary units and the interpretation of the components of the observed spectrum.

PANORAMIC EMISSION SPECTRA OF AIR

The model air mixture consisted of 80% N_2 and 20% O_2. The mixture of gases was prepared beforehand in a special mixing vessel. The mixture preparation time was three days. The gas was supplied to the low-pressure chamber through the measuring vessel (the volume ratio between the vessel and the LPC was 1 : 100).

Figure 5 shows the spectral distribution of the emission intensity of a shock wave in the air mixture in absolute energy units at velocities from 6.5 to 7.2 km/s. The data represented in Fig. 5 were obtained by the normalization of data from Fig. 4 to the calibration sensitivity of the Lega camera (Fig. 3, curves *2*, *3*). The results represented in Fig. 5 are consistent with data obtained on other installations (for example, see [10, 11]). The data given in Fig. 4 show that, in the emission spectrum of the air mixture, the lines of the nitrogen atom at 120, 141, 149, and 174 nm, a resonance line of the oxygen atom at 130 nm, and three lines of the carbon atom at 156, 166, and 193 nm have noticeable intensities. The presence of the lines of carbon in the spectrum of the air mixture can be explained by the diffusion of this element from the walls of the shock tube. Furthermore, structures characteristic of the emission of diatomic molecules were present in the test spectrum. Thus, emission in a wavelength range of 150–260 nm with a maximum at 190 nm belongs to the NO molecule, and emission in a range of 350–420 nm with a maximum at 387 nm belongs to the CN molecule; the emission of the N_2^+ ions can appear in the same region (387 nm).

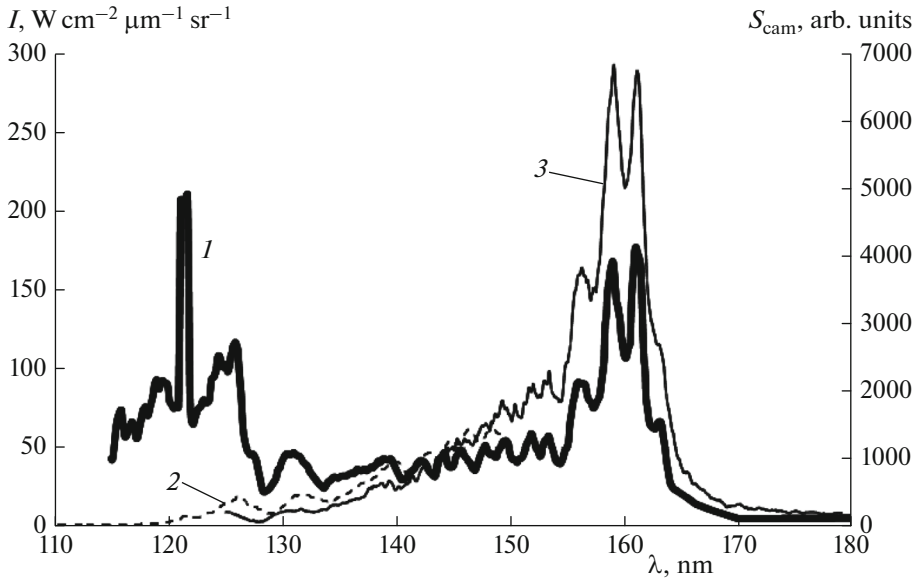

Fig. 3. (*1*) Spectral radiance of deuterium lamp emission in absolute energy units and (*2, 3*) emission spectra measured with the Lega camera in a range of 110–180 nm.

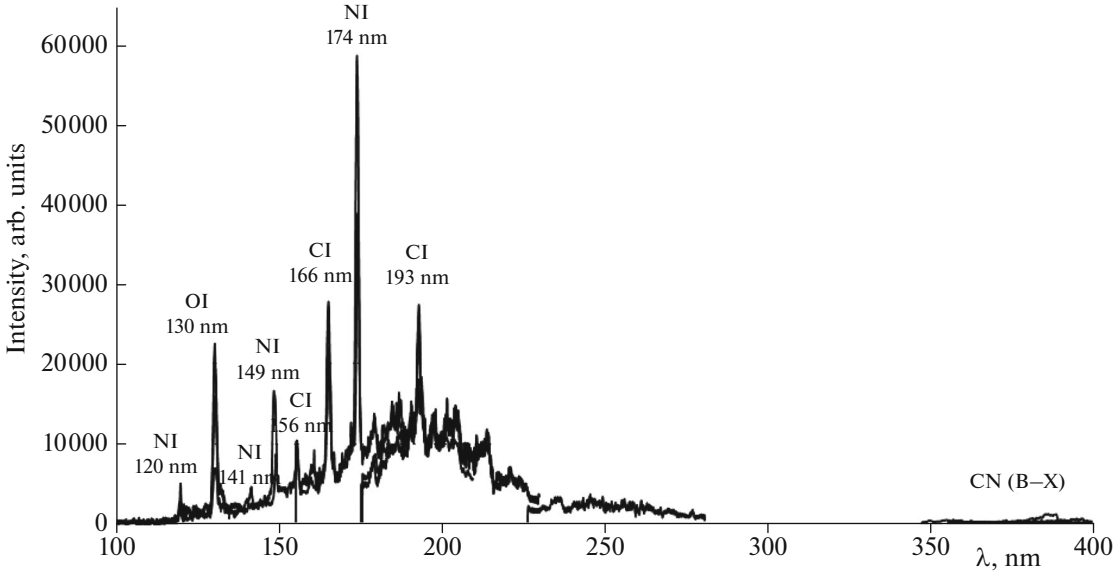

Fig. 4. Emission spectra of the air mixture in a shock wave at the initial pressure $p_1 = 0.25$ Torr in the low-pressure chamber. The shock wave velocity was 7.0–8.4 km/s.

Comparing the results obtained with experimental data on the radiant density of a shock wave in the visible region [3], we can make a conclusion on the noticeable contribution of emission in the VUV region to the total radiation flux at shock wave velocities higher than 6 km/s. Figure 6 demonstrates the strong dependence of the intensity of emission on shock wave velocity based on an example of a resonance line of the oxygen atom.

THE TIME DEPENDENCE OF THE EMISSION OF AIR BEHIND THE SHOCK WAVE FRONT

The experiments on studying the time characteristics of shock wave emission were carried out on the same optical system that was used for the measurement of panoramic spectra. In this case, a photomultiplier tube served as a radiation detector, and a unit with the exit slit was mounted at the output of the VM-1 monochromator. The widths of the entrance and exit

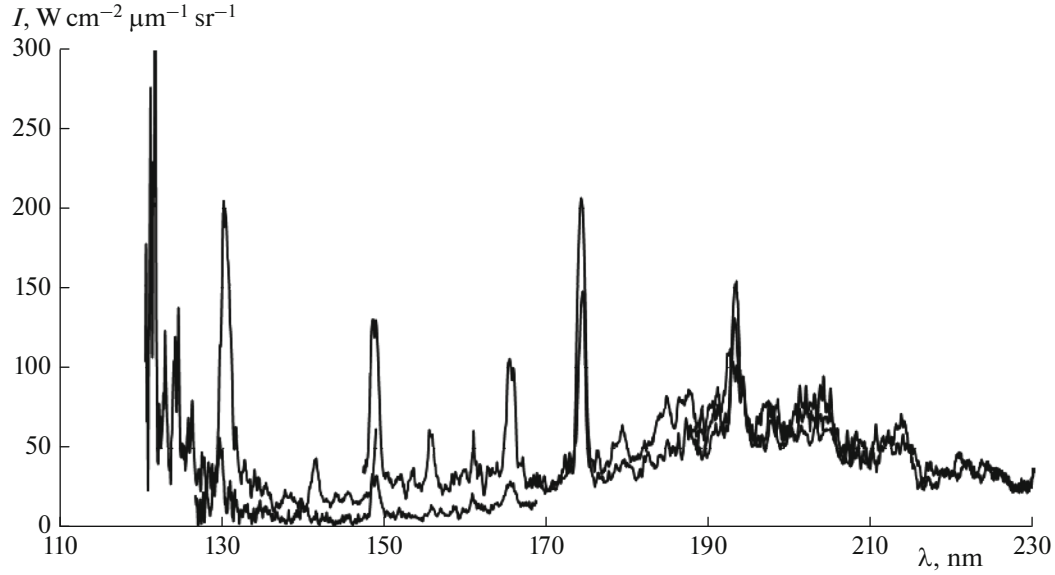

Fig. 5. Spectral radiant density of a shock wave in the air mixture in a spectral range of 115–230 nm at $p_1 = 0.25$ Torr. The shock wave velocity was 6.5–8.2 km/s.

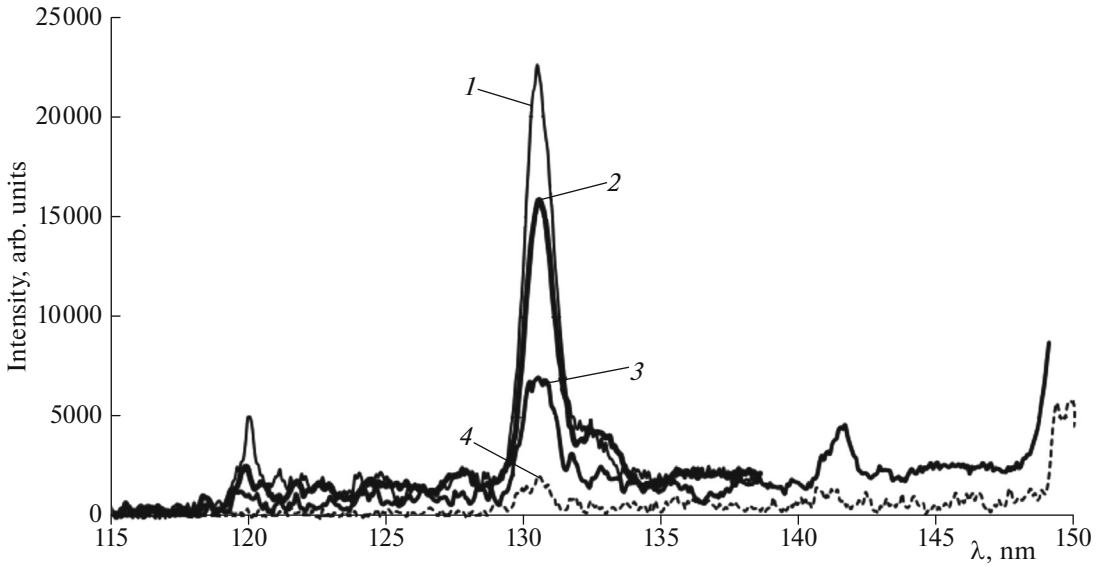

Fig. 6. Changes is the radiation intensity of a line of the oxygen atom at a wavelength of 130 nm at different shock wave velocities in air at $p_1 = 0.25$ Torr: $V =$ (*1*) 8.2, (*2*) 7.8, (*3*) 7.2, and (*4*) 6.5 km/s. The intensity is given in arbitrary units.

slits of the monochromator were 0.1 and 0.3 mm, respectively. Under these conditions, the width of the measured spectral range was 1 nm. A Hamamatsu 6836 photomultiplier tube was used in the experiments. The load resistance of the photomultiplier tube was 1 kΩ; in this case, the time constant of the metering circuit was no higher than 200 ns. The signal from the photomultiplier tube was measured with an Agilent DSO5014A 100-MHz oscilloscope.

The same deuterium lamp that was used in the study of panoramic spectra was used for the calibration of radiation detected by the photomultiplier tube in absolute energy units. The geometry of the optical calibration system remained unchanged. The calibration function of the optical system was determined with the aid of the results of calibration measurements. A graph of the dependence of the multiplier gain on the supply voltage was also obtained.

Based on the data of the panoramic emission spectra of the air mixture, we measured the time distributions of emission intensity in the wavelength range that corresponds to easily observed atomic lines and in the emission region of the NO molecule. The time distributions of emission intensity behind the shock wave

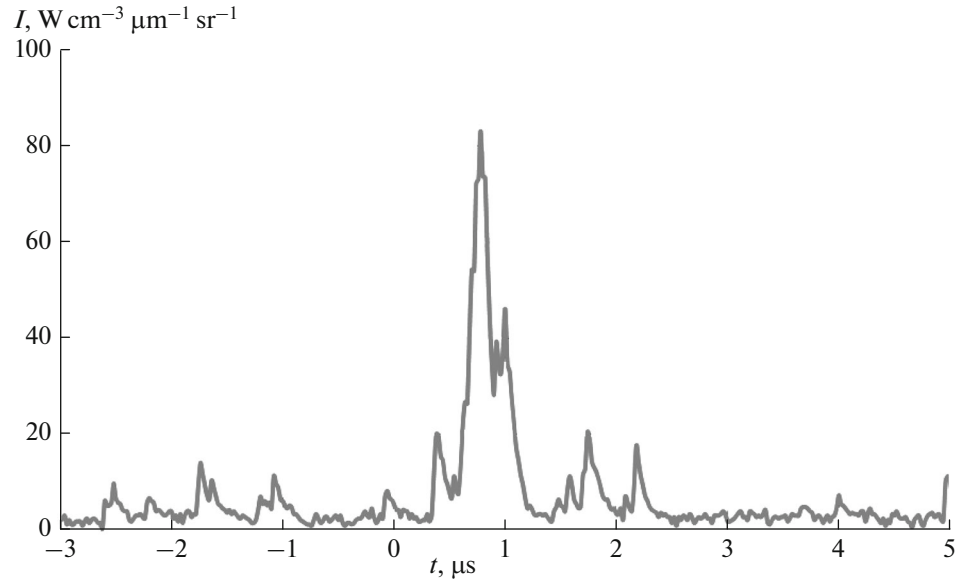

Fig. 7. The time dependence of the emission of the air mixture in a shock wave at a wavelength of 130 nm (a resonance line of the oxygen atom). Experimental conditions: $p_1 = 0.25$ Torr, and $V = 7.34$ km/s.

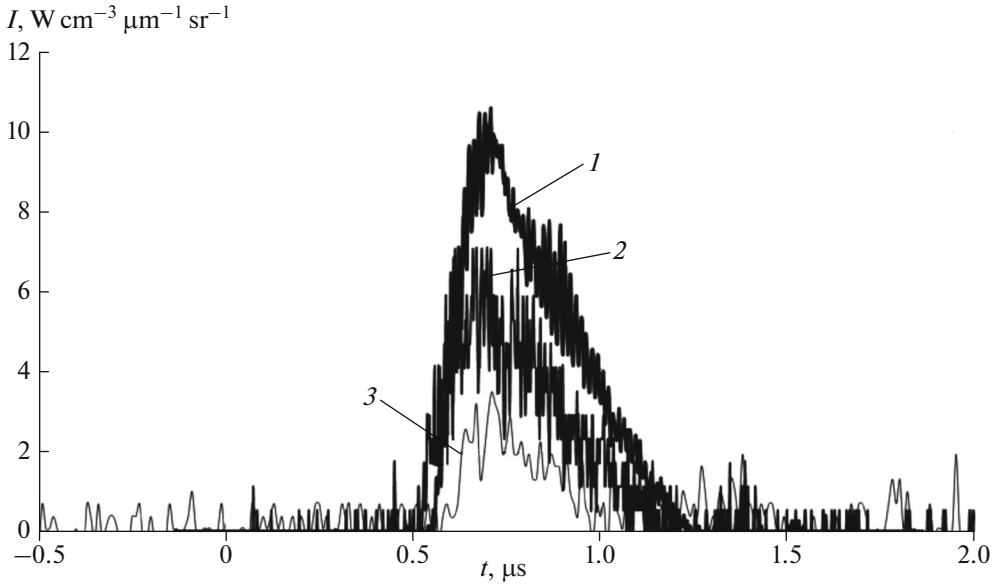

Fig. 8. The time dependence of shock wave emission in the air mixture at a wavelength of 174.5 nm (a line of the nitrogen atom) and $p_1 = 0.25$ Torr: $V =$ (*1*) 8.39, (*2*) 7.62, and (*3*) 7.45 km/s.

front were obtained in the mixtures of 80% N_2 + 20% O_2 at the initial pressure $p_1 = 0.25$ Torr and the shock wave velocities $V = 6.98$–8.49 km/s. Figures 7 and 8 show the corresponding time distributions for the atoms of oxygen and nitrogen, respectively.

CONCLUSIONS

In this work, we obtained quantitative data on the intensity and time evolution of the emission of air behind shock wave fronts in a spectral range of 120–400 nm at shock wave velocities of 6.3–8.4 km/s. A comparison of the emission intensity in the short-wavelength region of the spectrum (120–230 nm) with the emission in a range of 230–400 nm indicated a much higher radiation flux level in the short-wavelength region over the entire test temperature range. In this case, the strong dependence of the intensity of emission on the velocity of shock waves and, hence, on the temperature behind the shock wave front was observed. It was found that the observed duration of emission behind a shock wave in air at a pressure of

0.25 Torr before the wave front was about 1 μs at all of the test velocities of shock waves and over the entire test spectral range. The intensity of emission in the atomic lines of N and O at 120, 130, 141, and 149 nm was substantially higher than the background emission, which can be attributed to emission in the weaker lines of atoms and atomic ions or to bremsstrahlung emission.

With the use of the found time dependences of the intensity of emission, it should be taken into account that these results were obtained on a laboratory time scale. On going from the laboratory coordinate system to the intrinsic coordinate system of radiating gas, it is necessary to understand that gas compressed after a shock effect moves more slowly than the front in accordance with the jump of density.

The above results form a basis for the analysis of kinetic processes in air at temperatures of 30000–50000 degrees and for the calculation of the reliable rate constants of these processes instead of currently used models.

REFERENCES

1. J. H. Grinstead, M. C. Wilder, J. Olejniczak, et al., in *Proc. of the 46th AIAA Aerospace Sciences Meeting and Exhibit, Reno, Nevada* (AIAA, 2008), Paper No. 2008-1244.
2. B. A. Cruden, R. Martinez, J. H. Grinstead, and J. Olejniczak, in *Proc. of the 41st AIAA Thermophysics Conference, San Antonio, TX* (AIAA, 2009), Paper No. 2009-4240.
3. P. V. Kozlov and Yu. V. Romanenko, Fiz. Khim. Kinet. Gaz. Din. **15**, 221 (2014). http://chemphys.edu.ru/issues/2014-15-2/articles/221/
4. C. O. Johnston, in *Proc. of the 46th AIAA Aerospace Sciences Meeting and Exhibit, Reno, Nevada* (AIAA, 2008), Paper No. 2008-1245.
5. U. A. Sheikh, R. G. Morgan, and T. J. McIntyre, AIAA J. **53**, 3589 (2015).
6. J. Shang and S. Surzhikov, Prog. Aerospace Sci. **53**, 46 (2012).
7. A. M. Brandis, C. Johnston, and B. Cruden, and D. K. Prabhu, in *Proc. of the 43rd AIAA Thermophysics Conference, New Orleans, Louisiana* (AIAA, 2012), Paper No. 2012–2865.
8. S. Surzhikov, J. Chem. Phys. **398**, 56 (2012).
9. C. T. Surzhikov and M. P. Shuvalov, High Temp. **51**, 408 (2013).
10. A. M. Brandis, C. O. Johnston, B. A. Cruden, D. Prabhu, and D. Bose, J. Thermophys. Heat Transfer **29**, 209 (2015).
11. T. A. Hermann, F. Zander, H. Fulge, S. Loehle, and S. Fasoulas, in *Proc. of the 45th AIAA Plasmadynamics and Lasers Conference, Reston, VA* (AIAA, 2014), Paper No. 2014–2536.

Translated by V. Makhlyarchuk